Research in Astron. Astrophys. **2009** Vol. **9** No. **9**, 1049–1060
http://www.raa-journal.org *http://www.iop.org/journals/raa*

***R**esearch in*
***A**stronomy and*
***A**strophysics*

Poynting-Robertson effect on the linear stability of equilibrium points in the generalized photogravitational Chermnykh's problem

Badam Singh Kushvah

Department of Applied Mathematics, Indian School of Mines University, Dhanbad -826004, India; *bskush@gmail.com*

Received 2008 December 14; accepted 2009 June 6

Abstract The Poynting-Robertson (P-R) effect on linear stability of equilibrium points is investigated in the generalized photogravitational Chermnykh's problem when a bigger primary is radiating and a smaller primary is an oblate spheroid. The positions of equilibrium points and their linear stabilities for various values of perturbing parameters are studied. It is found that the positions of the equilibrium points are different from the positions in the classical restricted three body problem. When the P-R effect is taken into account, these points are unstable in a linear sense. It is also found that the equilibrium points are unstable when the mass of the belt $M_{\rm b} \geq 0.4$.

Key words: celestial mechanics

1 INTRODUCTION

The Chermnykh's problem is a new kind of restricted three body problem which was studied for the first time by Chermnykh (1987). This problem generalizes two classical problems of celestial mechanics: the two fixed center problem and the restricted three body problem. This gives wide perspectives for applications of the problem in celestial mechanics and astronomy. Goździewski (1998) studied the nonlinear stability of the Lagrangian libration points in the Chermnykh problem. The importance of the problem in astronomy has been addressed by Jiang & Yeh (2004). In their study, they have discussed many new discoveries of extrasolar planets which have been made recently and these events provide exciting and important opportunities to understand the formation and evolution of planetary systems, including the Solar System. There are similarities between extrasolar planets and planets in our Solar System. Some planetary systems are claimed to have disks of dust and they are regarded as young analogs of the Kuiper Belt in our Solar System. If these disks are massive enough, they should play important roles in the origin of planets' orbital elements. Since the belt of planetesimals often exists within a planetary system and provides the possible mechanism for orbital circularization, it is important to understand the solutions of dynamical systems which show planet-belt interactions.

The numerical exploration of the Chermnykh's problem has been presented by Papadakis (2005) in which the equilibrium points and zero velocity curves are studied numerically, and also the non-linear stability for the triangular Lagrangian points is computed for the Earth-Moon and Sun-Jupiter mass distribution with varying angular velocities. Jiang & Yeh (2006) and Yeh & Jiang (2006) examined the conditions for the existence of equilibrium points in the Chermnykh-like problems for different values of mass parameter μ. They have included the potential of the belt, and found three collinear points, two triangular points, and two other new equilibrium points. Papadakis & Kanavos (2007) presented the numerical exploration of the photogravitational restricted five-body problem. They have found that

the number of collinear equilibrium points in the problem depends on the mass parameter β and the radiation factors $q_i, i = 0, \ldots 3$. They have also given critical masses associated with the number of equilibrium points and their stability.

This paper highlights the generalization of Chermnykh's problem by including the Poynting-Robertson (P-R) effect which occurs because of grains of dust or small particles that absorb energy preferentially from one direction (i.e., the Sun), but re-emit the energy equally in all directions. The P-R effect operates by sweeping small particles from the solar system into the Sun at a cosmically rapid rate. Poynting (1903) considered the effect of absorption and subsequent re-emission of sunlight by small isolated particles in the solar system. That work was modified by Robertson (1937), using precise relativistic treatments of the first order in the ratio $\frac{\boldsymbol{V}}{\boldsymbol{c}}$ of the velocity of the particle to that of light. Taking into account the radiation pressure and the P-R drag force, Chernikov (1970) discussed the position as well as the stability of Lagrangian equilibrium points. Murray (1994) systematically discussed the dynamical effect of general drag in the planar circular restricted three body problem. Ishwar & Kushvah (2006) examined the linear stability of triangular equilibrium points in the generalized photogravitational restricted three body problem with P-R drag and found that the L_4 and L_5 points became unstable due to P-R drag. This is very remarkable and important, because they are linearly stable in classical problems when $0 < \mu < \mu_{\rm Routh} = 0.0385201$. Further, the normalizations of the Hamiltonian and the nonlinear stability of $L_{4(5)}$ in the presence of P-R drag have been studied by Kushvah et al. (2007a,b,c).

2 EQUATIONS OF MOTION

In this work, a Sun-Jupiter system of primaries is studied in which the mass of the Sun $m_1 \approx 1.989 \times 10^{30}$ kg and the mass of the Jupiter $m_2 \approx 1.8986 \times 10^{27}$ kg. It is supposed that the motion of an infinitesimal mass particle is influenced by the gravitational force from primaries and a belt of mass $M_{\rm b}$. Let Ox and Oy be in the equatorial plane of the smaller primary, Oz coincide with the polar axis of m_2 and the infinitesimal mass m be placed at the point $P(x, y, 0)$. The units of mass, distance and time are taken such that the sum of the masses and the distance between the primaries are unities, the Gaussian constant of gravitation $\Bbbk^2 = 1$. Then the perturbed mean motion n of the primaries is given by $n^2 = 1 + \frac{3A_2}{2} + \frac{2M_{\rm b}r_c}{(r_c^2+T^2)^{3/2}}$, where $T = a + b$, and a, b are flatness and core parameters respectively, which determine the density profile of the belt, $r_c^2 = (1-\mu)q_1^{2/3} + \mu^2$, $A_2 = \frac{r_{\rm e}^2 - r_{\rm p}^2}{5r^2}$ is the oblateness coefficient of m_2; $r_{\rm e}$ and $r_{\rm p}$ are the equatorial and polar radii of m_2 respectively, r is the distance between primaries, $\mu = \frac{m_2}{m_1+m_2}$($9.537 \times 10^{-4}$ for the Sun-Jupiter mass distribution) is the mass parameter, $q_1 = 1 - \frac{F_{\rm p}}{F_{\rm g}}$ is a mass reduction factor and $F_{\rm p}$ is the solar radiation pressure force which is exactly apposite to the gravitational attraction force $F_{\rm g}$. The coordinates of m_1 and m_2 are $(-\mu, 0)$ and $(1-\mu, 0)$ respectively. The dimensionless velocity of light is $c_{\rm d} = c = 299\,792\,458$ which depends on the physical masses of the two primaries and the distance between them. In the above mentioned reference system, the equations of motion of the infinitesimal mass particle in the xy-plane are formulated by using the following perturbation force [please see Robertson (1937); Chernikov (1970)]:

$$\boldsymbol{F} = \boldsymbol{F}_1 + \boldsymbol{F}_2 + \boldsymbol{F}_3, \tag{1}$$

where $\boldsymbol{F}_1 = F_{\rm p}\frac{\boldsymbol{R}}{R}$, $\boldsymbol{F}_2 = -F_{\rm p}\left(\frac{\boldsymbol{V}\cdot\boldsymbol{R}}{cR}\right)\frac{\boldsymbol{R}}{R}$, $\boldsymbol{F}_3 = -F_{\rm p}\frac{\boldsymbol{V}}{c}$, $\boldsymbol{R}$ is the position vector of P with respect to the radiating primary Sun S, and $\boldsymbol{V}$ is the corresponding velocity vector.

In Equation (1), $\boldsymbol{F}_1$ represents the radiation pressure, $\boldsymbol{F}_2$ represents the Doppler shift of the incident radiation and the $\boldsymbol{F}_3$ term is due to the absorption and subsequent re-emission of the incident radiation. The components $\boldsymbol{F}_2$ and $\boldsymbol{F}_3$ taken together give the P-R effect.

Considering the model proposed by Miyamoto & Nagai (1975), the potential of the belt is given by the density profile:

$$\rho(r,z) = \left(\frac{b^2 M_{\rm b}}{4\pi}\right)\frac{ar^2 + \left(a + 3\sqrt{z^2+b^2}\right)\left(a+\sqrt{z^2+b^2}\right)^2}{\left[r^2 + \left(a+\sqrt{z^2+b^2}\right)^2\right]^{5/2}\left(z^2+b^2\right)^{3/2}}, \tag{2}$$

where $M_{\rm b}$ is the total mass of the belt and $r^2 = x^2 + y^2$. The potential of the belt in the xy-plane is:

$$V(r,0) = -\frac{M_{\rm b}}{\sqrt{r^2+T^2}}. \tag{3}$$

Using Equations (1) and (3), the equations of motion are given (Kushvah 2008a,b) as:

$$\ddot{x} - 2n\dot{y} = \Omega_x, \tag{4}$$

$$\ddot{y} + 2n\dot{x} = \Omega_y, \tag{5}$$

where

$$\begin{aligned}
\Omega_x &= n^2 x - \frac{(1-\mu)q_1(x+\mu)}{r_1^3} - \frac{\mu(x+\mu-1)}{r_2^3} - \frac{3}{2}\frac{\mu A_2(x+\mu-1)}{r_2^5} \\
&\quad - \frac{M_{\rm b}x}{(r^2+T^2)^{3/2}} - \frac{W_1}{r_1^2}\left\{\frac{(x+\mu)}{r_1^2}[(x+\mu)\dot{x}+y\dot{y}] + \dot{x} - ny\right\}, \\
\Omega_y &= n^2 y - \frac{(1-\mu)q_1 y}{r_1^3} - \frac{\mu y}{r_2^3} - \frac{3}{2}\frac{\mu A_2 y}{r_2^5} \\
&\quad - \frac{M_{\rm b}y}{(r^2+T^2)^{3/2}} - \frac{W_1}{r_1^2}\left\{\frac{y}{r_1^2}[(x+\mu)\dot{x}+y\dot{y}] + \dot{y} + n(x+\mu)\right\},
\end{aligned}$$

$$\begin{aligned}
\Omega &= \frac{n^2(x^2+y^2)}{2} + \frac{(1-\mu)q_1}{r_1} + \frac{\mu}{r_2} + \frac{\mu A_2}{2r_2^3} + \frac{M_{\rm b}}{(r^2+T^2)^{1/2}} \\
&\quad + W_1\left[\frac{(x+\mu)\dot{x}+y\dot{y}}{2r_1^2} - n\arctan\left(\frac{y}{x+\mu}\right)\right], \\
W_1 &= \frac{(1-\mu)(1-q_1)}{c_d}.
\end{aligned}$$

From Equations (4) and (5), the energy integral is given below as:

$$C = 2\Omega - \dot{x}^2 - \dot{y}^2, \tag{6}$$

where the quantity C is Jacobi's constant.

3 POSITIONS OF EQUILIBRIUM POINTS

The orbital plane Oxy is divided into three parts $x \le -\mu$, $-\mu < x < 1-\mu$ and $1-\mu \le x$ with respect to the primaries. For simplicity, $\mu = 9.537 \times 10^{-4}$, $T = 0.01$, and $c = 299\,792\,458$ are used for numerical calculations.

The equilibrium points are given by substituting $\Omega_x = \Omega_y = 0$, i.e.

$$n^2 x - \frac{(1-\mu)q_1(x+\mu)}{r_1^3} - \frac{\mu(x+\mu-1)}{r_2^3} - \frac{3}{2}\frac{\mu A_2(x+\mu-1)}{r_2^5} - \frac{M_{\rm b}x}{(r^2+T^2)^{3/2}} + \frac{W_1 ny}{r_1^2} = 0, \tag{7}$$

$$n^2 y - \frac{(1-\mu)q_1 y}{r_1^3} - \frac{\mu y}{r_2^3} - \frac{3}{2}\frac{\mu A_2 y}{r_2^5} - \frac{M_{\rm b}y}{(r^2+T^2)^{3/2}} - \frac{W_1 n(x+\mu)}{r_1^2} = 0. \tag{8}$$

From Equations (7) and (8), we obtained:

$$r_1 = q_1^{1/3}\left\{1 - \frac{nW_1}{6(1-\mu)y} - \frac{A_2}{2} + \frac{(1-2r_c)M_{\rm b}\left[1 - \frac{3\mu A_2}{2(1-\mu)}\right]}{3\left(r_c^2+T^2\right)^{3/2}}\right\}, \tag{9}$$

$$r_2 = 1 + \frac{\mu(1-2r_c)M_{\rm b}}{3\left(r_c^2+T^2\right)^{3/2}} + \frac{nW_1}{3\mu y}, \tag{10}$$

$$x = -\mu \pm \left\{ \left(\frac{q_1}{n^2}\right)^{2/3} \left[1 + \frac{nW_1}{2(1-\mu)y} + \frac{3A_2}{2} - \frac{(1-2r_c)M_{\rm b}\left(1 - \frac{3\mu A_2}{2(1-\mu)}\right)}{\left(r_c^2+T^2\right)^{3/2}}\right]^{-2/3} - y^2 \right\}^{1/2}, \quad (11)$$

$$x = 1 - \mu \pm \left\{ \left[1 - \frac{nW_1}{\mu y}(1 - \frac{5}{2}A_2) - \frac{\mu(1-2r_0)M_{\rm b}}{\left(r_c^2+T^2\right)^{3/2}}\right]^{-2/3} - y^2 \right\}^{1/2}. \quad (12)$$

The equilibrium points $L_{4(5)}$ (the triangular equilibrium points in a classical case) are given by $\Omega_x = \Omega_y = 0; y \neq 0$. From Equations (4) and (5), the positions of $L_{4(5)}$ are given as follows:

$$x = -\mu + \frac{q_1^{2/3}}{2}(1 - A_2) - \frac{nW_1\left[\mu q_1^{2/3} - 2(1-\mu)\right]}{6\mu(1-\mu)y_0} + \frac{(1-2r_c)M_{\rm b}\left\{\left[1 - \frac{3\mu A_2}{(1-\mu)}\right] q_1^{2/3} - 1\right\}}{3\left(r_c^2+T^2\right)^{3/2}}, \quad (13)$$

$$y = \pm\frac{q_1^{1/3}}{2}\left\{4 - q_1^{2/3} + 2\left(q_1^{2/3} - 2\right)A_2 - \frac{2nW_1\left(q_1^{2/3} - 2\right)}{3\mu(1-\mu)y_0} - \frac{4(2r_c - 1)M_{\rm b}\left[\left(q_1^{2/3} - 3\right) - \frac{3\mu A_2\left(q_1^{2/3} - 3\right)}{2(1-\mu)}\right]}{3\left(r_c^2+T^2\right)^{3/2}}\right\}^{1/2}. \quad (14)$$

3.1 Positions of L_1 and $L_{4(5)}$

Using an iteration process, the positions of L_1 and $L_{4(5)}$ in region $(-\mu, 1-\mu)$ are obtained. The possible values of coordinates x and y of L_1 are presented in Table 1, and the corresponding plots are given in Figure 1 and frame (a) of Figure 2 for various values of $A_2, M_{\rm b}$ and q_1. In the classical case ($q_1 = 1, A_2 = 0, M_{\rm b} = 0$) abscissa $x = 0.93237$, ordinate $y = 0$; so L_1 lies on the x–axis. In other cases, the abscissa x decreases with the mass of the belt $M_{\rm b}$, the oblateness coefficient A_2 and the radiation pressure increase (i.e. q_1 decreases and the P-R effect is taken into account), while the ordinate y is negative lying below the line joining two primaries. It is found that y decreases when $M_{\rm b}$, A_2 and the radiation pressure increase. The possible values of x and y for the equilibrium point L_4 are given in Table 2, and the corresponding curves are presented in Figure 1 and in frame (d) of Figure 2. In the classical case, it has been observed that the coordinates $(x, y) = (0.499046, \pm 0.866025)$ of the triangular equilibrium points for the Sun-Jupiter mass distribution. When q_1 decreases (the P-R effect increases) then x and y decrease (i.e. when the P-R effect is very high then $L_{4(5)}$ coincides with the Sun). The positions of these points are no longer triangular.

3.2 Positions of L_2

When $x \in (1-\mu, \infty)$ all the possible values of x and y for L_2 are presented in Table 3, and the corresponding plots are given in Figure 1 and frame (b) of Figure 2 for various values of $A_2, M_{\rm b}$, and q_1. In the classical case ($q_1 = 1, A_2 = 0, M_{\rm b} = 0$), the abscissa $x = 1.06883$, ordinate $y = 0$; and in other cases, y is negative which lies below the line joining two primaries. The abscissa x increases and the ordinate y decreases when A_2 increases, while x and y decrease when $M_{\rm b}$ increases and q_1 decreases.

Table 1 Positions of L_1 when $T = 0.01, c = 299\,792\,458, \mu = 9.537 \times 10^{-4}$

		$M_b = 0.0$		$M_b = 0.2$		$M_b = 0.4$	
A_2	q_1	x	y	x	y	x	y
0.0	1.0	0.93237	0.0	0.916738	0.0	0.900954	0.0
	0.75	0.884161	-1.32662×10^{-9}	0.865462	-2.47036×10^{-9}	0.852505	-3.70164×10^{-9}
	0.50	0.785873	-1.70904×10^{-8}	0.787977	-1.96215×10^{-8}	0.789182	-2.18655×10^{-8}
	0.25	0.626836	-1.42486×10^{-7}	0.682241	-1.01072×10^{-7}	0.709627	-8.66699×10^{-8}
0.50	1.0	0.775012	0.0	0.776826	0.0	0.778294	0.0
	0.75	0.72677	-2.10496×10^{-9}	0.73634	-1.96187×10^{-9}	0.743233	-1.87805×10^{-9}
	0.50	0.647546	-1.43508×10^{-8}	0.675909	-1.06294×10^{-8}	0.694216	-8.74871×10^{-8}
	0.25	0.518629	-9.47861×10^{-8}	0.588491	-4.9532×10^{-8}	0.627896	-3.34487×10^{-8}

Table 2 Positions of L_4 when $T = 0.01, c = 299\,792\,458, \mu = 9.537 \times 10^{-4}$

		$M_b = 0.0$		$M_b = 0.2$		$M_b = 0.4$	
A_2	q_1	x	y	x	y	x	y
0.0	1.0	0.499046	0.866025	0.499046	0.807757	0.499046	0.771992
	0.75	0.411787	0.809399	0.417404	0.772863	0.420608	0.751208
	0.50	0.314026	0.728525	0.313985	0.728636	0.343182	0.715491
	0.25	0.19747	0.597895	0.313863	0.608757	0.34489	0.622967
0.50	1.0	0.343352	0.755027	0.344046	0.747635	0.344532	0.742483
	0.75	0.283264	0.698324	0.281106	0.707572	0.279649	0.713786
	0.50	0.215945	0.621895	0.200455	0.65786	0.190387	0.680385
	0.25	0.135683	0.504585	0.0642497	0.590149	0.0210436	0.633638

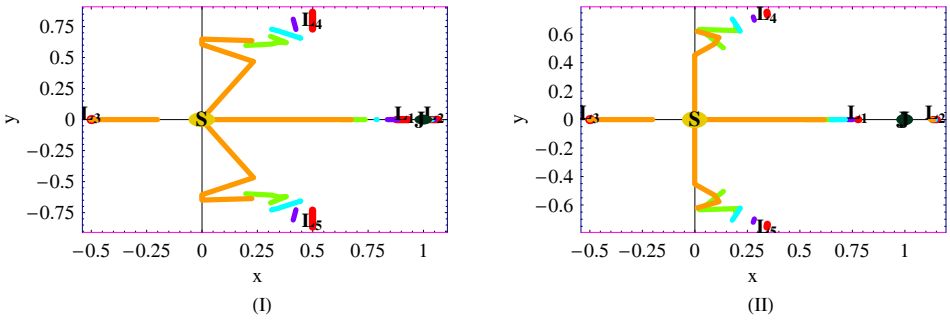

Fig. 1 Positions of equilibrium points when $\mu = 9.537 \times 10^{-4}, T = 0.01, c = 299\,792\,458, M_b = 0.0 - 0.8$, where the colors indicate different values of q_1 as red: 1.0, blue-violet: 0.75, cyan: 0.50, lime: 0.25, dark-orange: 0.0, in frame (I) $A_2 = 0$ and (II) $A_2 = 0.5$.

3.3 Positions of L_3

For $x \in (-\infty - \mu)$, all the possible values of x and y for L_3 are presented in Table 4 and the corresponding plots are given in Figure 1 and frame (c) of Figure 2 for various values of A_2, M_b and q_1. It is found that for all values of parameters, the abscissa x has constant value –0.500954; so it is less affected by the parameters. Except for the classical case (where $y = 0$), y is positive. The ordinate y is a decreasing function of mass of the belt M_b. When the radiation pressure (the P-R effect) increases i.e. q_1 decreases and the oblateness coefficient A_2 increases, the ordinate y increases.

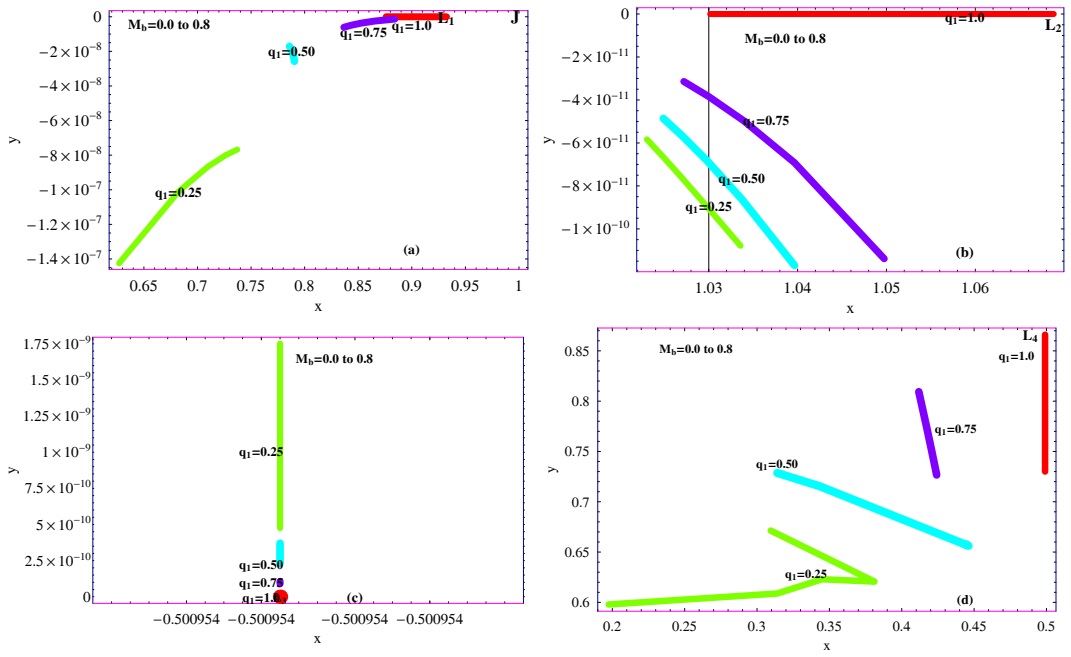

Fig. 2 Positions of equilibrium points when $\mu = 9.537 \times 10^{-4}, T = 0.01, c = 299\,792\,458, M_{\rm b} = 0.0 - 0.8, A_2 = 0$, where the colors indicate different values of q_1 as red: 1.0, blue-violet: 0.75, cyan: 0.50, lime: 0.25, first frame (a) for the positions of L_1, frame (b) for the positions of L_2, frame (c) for the positions of L_3, and frame (d) for the positions of L_4.

From the above results, it is observed that for the Sun-Jupiter mass distribution ($\mu = 9.537 \times 10^{-4}$) and for the radiation pressure coefficient $q_1 = 1$, the positions of equilibrium points $L_i (i = 1, 2, 3)$ lie on the x–axis line joining the primaries, for any values of $A_2, M_{\rm b}$ in [0,1). For $q_1 \neq 1$, the positions of L_1 and L_2 are displaced below the x–axis, but the position of L_3 is displaced up the line joining the primaries, and L_3 is less affected by A_2 and $M_{\rm b}$. In the classical case, the coordinates of $L_{4(5)}$ are $x = 0.499046 = \frac{1}{2} - \mu$, $y = \pm 0.866025 = \pm\frac{\sqrt{3}}{2}$. For $q_1 \neq 1$, the distances from the Sun to $L_{4(5)}$ decrease and from Jupiter they increase [i.e. when the P-R effect is very high, the test particle ultimately spirals into the radiating body (the Sun)]. All the above results are similar to the results of Szebehely (1967), Ragos & Zafiropoulos (1995) and Kushvah (2008a,b).

4 LINEAR STABILITY

In this section, the P-R effect on the linear stability conditions is examined. The notion of Lyapunov's stability occurs in the study of dynamical systems. In simple terms, if all solutions of the dynamical system that start out near an equilibrium point L_i $(i = 1, 2, 3, 4, 5)$ stay near L_i forever, then L_i is called Lyapunov stable. Let the position of any equilibrium point be (x^*, y^*) taking $x = x^* + \alpha$, $y = y^* + \beta$, where $\alpha = \xi e^{\lambda t}$, $\beta = \eta e^{\lambda t}$ are small displacements, and ξ, η, λ are parameters. Then, the equations of perturbed motion corresponding to the system of Equations (4) and (5) are as follows:

$$\ddot{\alpha} - 2n\dot{\beta} = \alpha\Omega^*_{xx} + \beta\Omega^*_{xy} + \dot{\alpha}\Omega^*_{x\dot{x}} + \dot{\beta}\Omega^*_{x\dot{y}}\,, \tag{15}$$

$$\ddot{\beta} + 2n\dot{\alpha} = \alpha\Omega^*_{yx} + \beta\Omega^*_{yy} + \dot{\alpha}\Omega^*_{y\dot{x}} + \dot{\beta}\Omega^*_{y\dot{y}}\,, \tag{16}$$

where superscript '$*$ 'corresponds to the equilibrium points.

$$(\lambda^2 - \lambda\Omega^*_{x\dot{x}} - \Omega^*_{xx})\xi + [-(2n + \Omega^*_{x\dot{y}})\lambda - \Omega^*_{xy}]\eta = 0, \tag{17}$$

$$[(2n - \Omega^*_{y\dot{x}})\lambda - \Omega^*_{yx}]\xi + (\lambda^2 - \lambda\Omega^*_{y\dot{y}} - \Omega^*_{yy})\eta = 0\,. \tag{18}$$

Equations (17) and (18) have singular solutions if,

$$\begin{vmatrix} \lambda^2 - \lambda\Omega^*_{x\dot{x}} - \Omega^*_{xx} & -(2n + \Omega^*_{x\dot{y}})\lambda - \Omega^*_{xy} \\ (2n - \Omega^*_{y\dot{x}})\lambda - \Omega^*_{yx} & \lambda^2 - \lambda\Omega^*_{y\dot{y}} - \Omega^*_{yy} \end{vmatrix} = 0\,.$$

From the above, we obtained the characteristic equation:

$$\lambda^4 + a\lambda^3 + b\lambda^2 + c\lambda + d = 0\,, \tag{19}$$

where

$$a = 3\frac{W_1}{r^2_{1*}}, \tag{20}$$

$$b = 2n^2 - f_* - \frac{3\mu A_2}{r^5_{2*}} + \frac{3M_bT^2}{(r^2_* + T^2)^{5/2}} + \frac{2W_1^2}{r^4_{1*}}, \tag{21}$$

$$c = -a(1 + e), \tag{22}$$

$$e = \frac{\mu}{r^5_{2*}}A_2 + \frac{\mu}{r^2_{1*}r^5_{2*}}\Big(1 + \frac{5A_2}{2r^2_{2*}}\Big)y^2_* + \frac{3M_b\left(\frac{\mu^2 y^2_*}{r^2_*} - T^2\right)}{(r^2_* + T^2)^{5/2}}, \tag{23}$$

Table 3 Positions of L_2 when $T = 0.01, c = 299\,792\,458, \mu = 9.537 \times 10^{-4}$

		$M_\mathrm{b} = 0.0$		$M_\mathrm{b} = 0.2$		$M_\mathrm{b} = 0.4$	
A_2	q_1	x	y	x	y	x	y
0.0	1.0	1.06883	0.0	1.04908	0.0	1.03964	0.0
	0.75	1.04975	-1.13857×10^{-10}	1.03965	-6.91819×10^{-11}	1.03386	-4.94368×10^{-11}
	0.50	1.03965	-1.16998×10^{-10}	1.03372	-8.61453×10^{-11}	1.02983	-6.83734×10^{-11}
	0.25	1.03357	-1.07833×10^{-10}	1.02966	-8.89477×10^{-11}	1.02686	-7.56684×10^{-11}
0.50	1.0	1.15428	0.0	1.14656	0.0	1.1405	0.0
	0.75	1.14932	-1.14631×10^{-10}	1.1426	-1.01356×10^{-10}	1.13722	-9.13642×10^{-11}
	0.50	1.14495	-1.98151×10^{-10}	1.13905	-1.79064×10^{-10}	1.13423	-1.63983×10^{-10}
	0.25	1.14107	-2.60133×10^{-10}	1.13584	-2.39457×10^{-10}	1.1315	-2.22313×10^{-10}

Table 4 Positions of L_3 , when $T = 0.01, c = 299\,792\,458, \mu = 9.537 \times 10^{-4}$

		$x = 0.500954$			
A_2	q_1	$y : M_\mathrm{b} = 0.0$	$y : M_\mathrm{b} = 0.2$	$y : M_\mathrm{b} = 0.4$	$y : M_\mathrm{b} = 0.6$
0.0	1.0	0.0	0.0	0.0	0.0
	0.75	1.06633×10^{-10}	1.02729×10^{-10}	19.81981×10^{-11}	9.38157×10^{-11}
	0.50	3.7017×10^{-10}	3.13147×10^{-10}	2.76314×10^{-10}	2.50019×10^{-10}
	0.25	1.75207×10^{-9}	9.40281×10^{-10}	6.83146×10^{-10}	5.54448×10^{-10}
0.50	1.0	0.0	0.0	0.0	0.0
	0.75	1.75825×10^{-10}	1.51585×10^{-10}	1.35055×10^{-10}	1.22896×10^{-10}
	0.50	6.87953×10^{-10}	4.94413×10^{-10}	3.96932×10^{-10}	3.37618×10^{-10}
	0.25	8.1313×10^{-9}	1.7223×10^{-9}	1.06253×10^{-9}	7.86714×10^{-10}

Table 5 Zero Velocity Curves when $T = 0.01, \mu = 0.025$

Frame	I ($q_1 = 1$) closed oval around $L_{4(5)}$ linearly stable	II ($q_1 = 0.5$) oval around $L_{4(5)}$, stability	III ($q_1 = 0.0$) $L_{4(5)}$, stability
A ($A_2 = 0.0, M_\mathrm{b} = 0$)	yes, the classical case	no oval, unstable	affected by radiation pressure
B ($A_2 = 0.5, M_\mathrm{b} = 0$)	yes, affected by the oblateness	no oval, unstable	unstable
C ($A_2 = 0.0, M_\mathrm{b} = 0.2$)	yes, affected by the belt	no oval, unstable	unstable
D ($A_2 = 0.5, M_\mathrm{b} = 0.2$)	affected by the belt, the oblateness	no oval, unstable	unstable

Table 6 Roots of the Characteristic Equation when $A_2 = 0.0, T = 0.01, r_c = 0.9999$, $c = 299\,792\,458$, $\mu = 9.537 \times 10^{-4}$

M_b	q_1	ω_1	ω_2
0.0	1.0	$0.0 \pm 0.137114\mathbf{i}$	$0.0 \pm 0.990555\mathbf{i}$
	0.75	$-1.52439 \times 10^{-9} \pm 0.141116\mathbf{i}$	$1.05214 \times 10^{-11} \pm 0.989993\mathbf{i}$
	0.50	$-3.99678 \times 10^{-9} \pm 0.145481\mathbf{i}$	$2.93194 \times 10^{-11} \pm 0.989362\mathbf{i}$
	0.25	$-9.521 \times 10^{-9} \pm 0.150542\mathbf{i}$	$7.47926 \times 10^{-11} \pm 0.988606\mathbf{i}$
	0.0	Indeterminate	Indeterminate
0.2	1.0	$0.0 \pm 0.646245\mathbf{i}$	$0.0 \pm 1.05546\mathbf{i}$
	0.75	1.29446	$-4.01728 \times 10^{-10} \pm 1.73126\mathbf{i}$
	0.50	1.60178	$-1.13096 \times 10^{-9} \pm 1.82678\mathbf{i}$
	0.25	2.04762	$-2.62876 \times 10^{-9} \pm 1.59591\mathbf{i}$
	0.0	Indeterminate	Indeterminate
0.4	1.0	$1.80764 \mp 2.09382\mathbf{i}$	$-1.80764 \pm 2.09382\mathbf{i}$
	0.75	5.7348	$-5.59117 \times 10^{-10} \pm 5.90277\mathbf{i}$
	0.50	2.13073	$-1.17407 \times 10^{-9} \pm 1.17407\mathbf{i}$
	0.25	2.17613	$-2.35604 \times 10^{-9} \pm 1.70915\mathbf{i}$
	0.0	Indeterminate	Indeterminate
0.6	1.0	$1.00792 \mp 1.58918\mathbf{i}$	$1.00792 \pm 1.58918\mathbf{i}$
	0.75	$1.05708 \mp 1.57568\mathbf{i}$	$1.05708 \pm 1.57568\mathbf{i}$
	0.50	$6.67049 \mp 6.74474\mathbf{i}$	$6.67049 \pm 6.74474\mathbf{i}$
	0.25	2.22229	$-2.15946 \times 10^{-9} \pm 1.97335\mathbf{i}$
	0.0	Indeterminate	Indeterminate

$$
\begin{aligned}
d \;=\; & (n^2 - f_*)\left[n^2 + 2f_* - \frac{3\mu A_2}{r_{2*}^5} + \frac{3M_\mathrm{b}T^2}{(r_*^2 + T^2)^{5/2}}\right] \\
& + 9\mu(1-\mu)y_*^2\left\{\frac{q_1}{r_{1*}^5 r_{2*}^5} + \frac{3M_\mathrm{b}}{(r_*^2+T^2)^{5/2}}\left[\frac{\mu q_1}{r_{1*}^5} + \frac{(1-\mu)\left(1+\frac{5A_2}{2r_{2*}^2}\right)}{r_{2*}^5}\right]\right\} \\
& - \frac{6\mu n W_1 y_*}{r_{1*}^4}\left\{\frac{(x_*+\mu)(x_*+\mu-1)+y_*^2}{r_{2*}^5} + \frac{3M_\mathrm{b}[x_*(x_*+\mu)+y_*^2]}{(r_*^2+T^2)^{5/2}}\right\}, \qquad (24)
\end{aligned}
$$

$$
f_* \;=\; \frac{(1-\mu)q_1}{r_{1_*}^3} + \frac{\mu}{r_{2*}^3}\left(1 + \frac{3}{2}\frac{A_2}{r_{2*}^2}\right) + \frac{3M_\mathrm{b}}{(r_*^2+T^2)^{5/2}}\,. \qquad (25)
$$

Taking $y \to 0, \frac{W_1}{y} \to 0$ because $y \gg W_1$ and $x \gg W_1$, from Equation (9), we have $r_1 \approx \left[\frac{q_1}{n^2}\right]^{1/3}$. At equilibrium points L_i $(i = 1, 2, 3)$, $f_* > 1$. Thus, the characteristic Equation (19) has roots with a positive real part, which shows that these points are unstable in a linear sense. The same results are shown in the zero velocity curves of Figure 3, where it is found that there is no closed curve (oval) around L_1, L_2 and L_3.

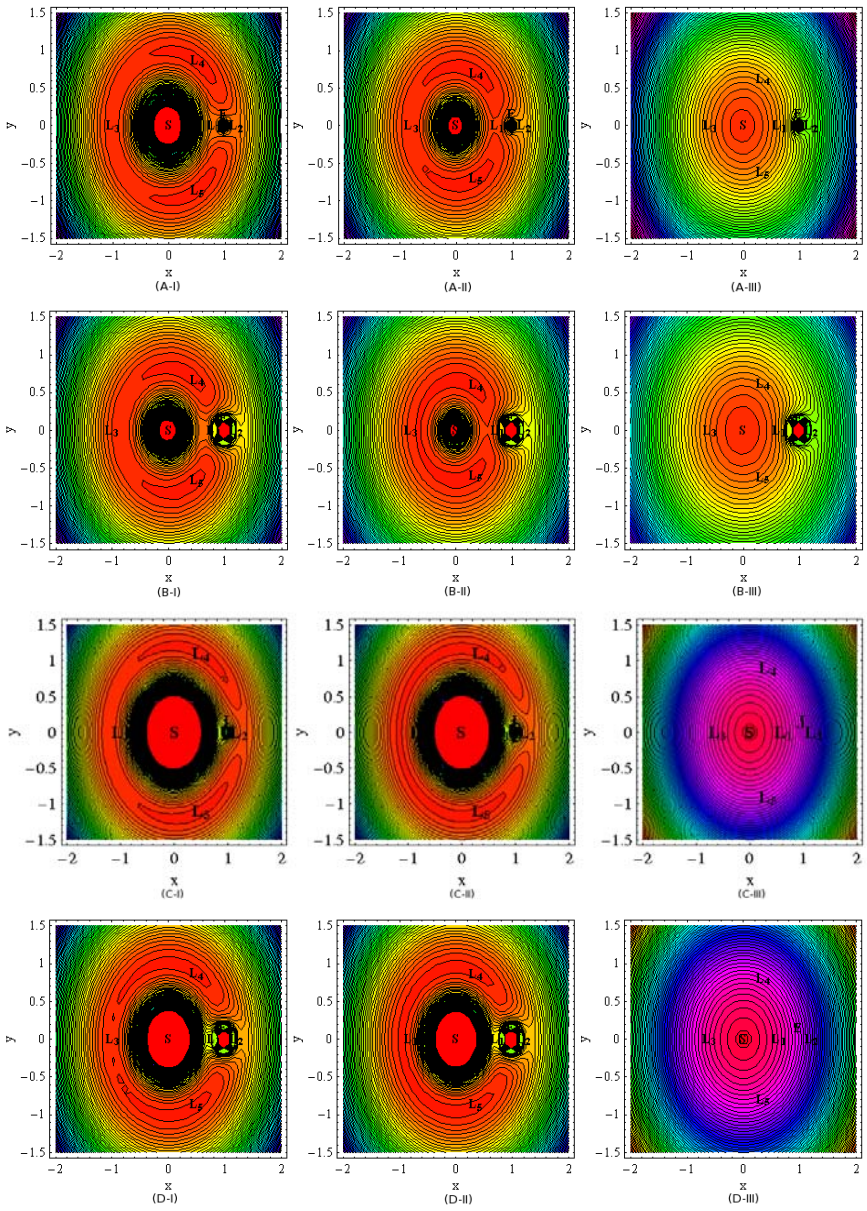

Fig. 3 Zero velocity curves for $\mu = 0.025, T = 0.01, r_c = 0.9999$, frames (A-I to III) $q_1 = 1, q_1 = 0.5, q_1 = 0.0, A_2 = 0.0, M_b = 0$, (B-I to III) $q_1 = 1, q_1 = 0.5, q_1 = 0.0, A_2 = 0.5, M_b = 0$, (C-I to III) $q_1 = 1, q_1 = 0.5, q_1 = 0.0, A_2 = 0.0, M_b = 0.2$, (D-I to III) $q_1 = 1, q_1 = 0.5, q_1 = 0.0, A_2 = 0.5, M_b = 0.2$.

Now, using Ferrari's theorem, the roots of characteristic Equation (19) are given as:

$$\lambda_{1,2} = -\frac{a\left(1+\sqrt{1+8\alpha_1}\right)}{4} \pm \sqrt{\frac{a^2\left(1+\sqrt{1+8\alpha_1}\right)}{16} - B_1}, \tag{26}$$

$$\lambda_{3,4} = -\frac{a\left(1-\sqrt{1+8\alpha_1}\right)}{4} \pm \sqrt{\frac{a^2\left(1-\sqrt{1+8\alpha_1}\right)}{16} - B_2}, \tag{27}$$

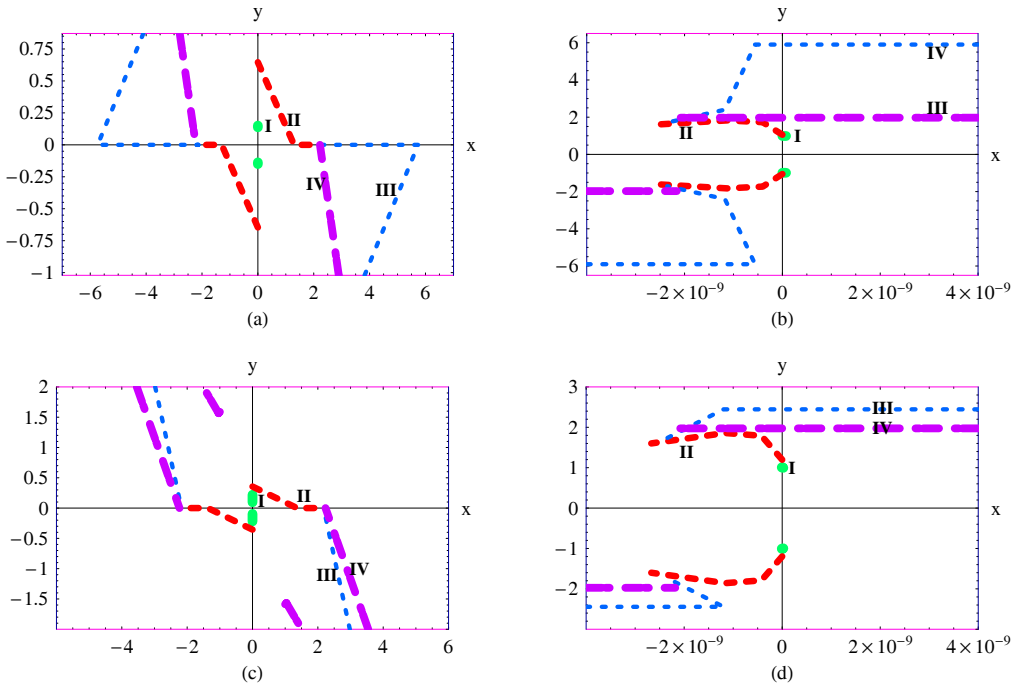

Fig. 4 xy-complex plane shows the values of ω_1 in frame (a) when $A_2 = 0$, in frame (c) when $A_2 = 0.02$ and the values of ω_2 in frame (b) when $A_2 = 0$, in frame (d) when $A_2 = 0.02$ curve labeled I: $M_b = 0.0$, II: $M_b = 0.2$, III: $M_b = 0.4$, IV: $M_b = 0.6$, for $\mu = 9.537 \times 10^{-4}, T = 0.01, r_c = 0.9999, c = 299\,792\,458, q_1 = 1.0$ to 0.0.

where

$$\alpha_1 = \frac{(1+e)(1+e^2-b)+d}{2(b^2-4d)} > 0,$$

$$B_1 = \left(\frac{b}{2} + \alpha_1 a^2\right)\left(1 + \sqrt{1+8\alpha_1}\right) - \frac{1+e}{\sqrt{1+8\alpha_1}},$$

$$B_2 = \left(\frac{b}{2} + \alpha_1 a^2\right)\left(1 - \sqrt{1+8\alpha_1}\right) + \frac{1+e}{\sqrt{1+8\alpha_1}}.$$

From the above Equations (26) and (27), the roots are $\lambda_{1,2} = \pm\omega_1$ are $\lambda_{3,4} = \pm\omega_2$; where ω_i $(i = 1, 2)$ are complex numbers (long/short -periodic frequencies), presented in Figure 4 in the xy-complex plane corresponding to Tables 6 and 7, and the corresponding curve plots of ω_1 are shown in frame (a) for $A_2 = 0$ and in frame (c) for $A_2 = 0.02$. The corresponding curve plots of ω_2 are shown in frame (b) for $A_2 = 0$ and in frame (d) for $A_2 = 0.02$. The curves, which are labeled I, II, III and IV, indicate different values of M_b as I: 0.0, II: 0.2, III: 0.4, IV: 0.6, for $\mu = 9.537 \times 10^{-4}, T = 0.01, c = 299\,792\,458$, $q_1 = 1.0 - 0.0$. It is found that for $A_2 = 0.0, 0.02, q_1 = 1, 0.0 \leq M_b < 0.4$, ω_i $(i = 1, 2)$ are purely imaginary, hence the triangular equilibrium points are conditionally stable in the Lyapunov sense. For $A_2 = 0.0, 0.02, q_1 \neq 1$ and $M_b = 0.4, 0.6$, ω_i $(i = 1, 2)$ are complex numbers having at least one positive real part, so $L_{4(5)}$ points are unstable in the linear sense. They are also unstable for $M_b \geq 0.4$ even if q_1 has any value in [0,1]. The stability of equilibrium points is less affected by the oblateness coefficient A_2. The same results are presented by the zero velocity curves $C = 2\Omega(x, y)$ in various frames of Figure 3 for the entire range of parameters q_1, A_2, and M_b (please see Table 5). It is found that for $q_1 = 1$, there are closed curves around $L_{4(5)}$ and the radiation pressure may increase the size

Table 7 Roots of the Characteristic Equation when $A_2 = 0.02, T = 0.01, r_c = 0.9999, c = 299\,792\,458, \mu = 9.537 \times 10^{-4}$

M_b	q_1	ω_1	ω_2
0.0	1.0	$0.0 \pm 0.0959401\mathbf{i}$	$0.0 \pm 1.01389\mathbf{i}$
	0.75	$-1.52674 \times 10^{-9} \pm 0.142645\mathbf{i}$	$-8.6941 \times 10^{-12} \pm 1.00904\mathbf{i}$
	0.50	$-4.01198 \times 10^{-9} \pm 0.181649\mathbf{i}$	$-8.08359 \times 10^{-12} \pm 1.00349\mathbf{i}$
	0.25	$-9.58469 \times 10^{-9} \pm 0.219817\mathbf{i}$	$2.35833 \times 10^{-11} \pm 0.996711\mathbf{i}$
	0.0	Indeterminate	Indeterminate
0.2	1.0	$0.0 \pm 0.355149\mathbf{i}$	$0.0 \pm 1.19752\mathbf{i}$
	0.75	1.36357	$-4.23604 \times 10^{-10} \pm 1.79011\mathbf{i}$
	0.50	1.63501	$-1.16304 \times 10^{-9} \pm 1.85862\mathbf{i}$
	0.25	2.06369	$-2.67091 \times 10^{-9} \pm 1.60078\mathbf{i}$
	0.0	Indeterminate	Indeterminate
0.4	1.0	$1.69572 \mp 2.00141\mathbf{i}$	$1.69572 \pm 2.00141\mathbf{i}$
	0.75	$3.7197 \mp 3.85022\mathbf{i}$	$3.7197 \pm 3.85022\mathbf{i}$
	0.50	2.17618	$-1.19613 \times 10^{-9} \pm 2.44471\mathbf{i}$
	0.25	2.19103	$-2.38507 \times 10^{-9} \pm 1.70955\mathbf{i}$
	0.0	Indeterminate	Indeterminate
0.6	1.0	$0.997688 \mp 1.5873\mathbf{i}$	$0.997688 \pm 1.5873\mathbf{i}$
	0.75	$1.03688 \mp 1.56591\mathbf{i}$	$1.03688 \pm 1.56591\mathbf{i}$
	0.50	$6.58926 \mp 6.66469\mathbf{i}$	$6.58926 \pm 6.66469\mathbf{i}$
	0.25	2.2346	$-2.18146 \times 10^{-9} \pm 1.9735\mathbf{i}$
	0.0	Indeterminate	Indeterminate

of the ovals, which implies that the instability range increases, i.e the region for oscillation of the points becomes very large. For very high radiation pressure, ovals disappear [please see (III) frames of Fig. 3] and the points can move freely in space, so they ultimately spiral into the Sun. The above results are similar to the results in Chernikov (1970) and Kushvah (2008b).

5 CONCLUSIONS

It has been found that the collinear points L_1, L_2 and L_3 no longer lie along the line joining the primaries and they are linearly unstable even in the classical case. The position of L_3 is less affected by the oblateness coefficient A_2. Because of the P-R effect, the $L_{4(5)}$ no longer remains in the triangular position with respect to the primaries. The $L_{4(5)}$ value is stable in a linear sense for the mass reduction factor $q_1 = 1$, mass of the belt M_b in $[0, 0.4)$ and any value of A_2 in [0,1). These points are linearly unstable due to the P-R effect ($q_1 \neq 1$) for all values of M_b, and A_2 in [0,1). Furthermore, it is observed that $L_{4(5)}$ are unstable in a linear sense for $M_\mathrm{b} \geq 0.4$ even if q_1 could assume any value in [0,1]. Thus, we conclude that the position and linear stability of equilibrium points are different from the classical restricted three body problem due to the P-R effect, influence from the belt and the oblateness effect of the second primary.

Acknowledgements I am thankful to Professor B. Ishwar, University Department of Mathematics, B. R. A. Bihar University Muzaffarpur (India) and Dr. Gorakh Nath, Department of Mathematics, NIT Raipur (India) for their valuable suggestions during revision of the manuscript.

References

Chermnykh, S. V. 1987, Leningradskii Universitet Vestnik Matematika Mekhanika Astronomiia, 73
Chernikov, Y. A. 1970, AZh, 47, 217
Goździewski, K. 1998, Celestial Mechanics and Dynamical Astronomy, 70, 41
Ishwar, B., & Kushvah, B. S. 2006, Journal of Dynamical Systems & Geometric Theories, 4(1), 79
Jiang, I.-G., & Yeh, L.-C. 2004, International Journal of Bifurcation and Chaos, 14, 3153
Jiang, I.-G., & Yeh, L.-C. 2006, Ap&SS, 305, 341
Kushvah, B. S. 2008a, Ap&SS, 318, 41
Kushvah, B. S. 2008b, Ap&SS, 315, 231
Kushvah, B. S., Sharma, J. P., & Ishwar, B. 2007a, Bulletin of the Astronomical Society of India, 35, 319
Kushvah, B. S., Sharma, J. P., & Ishwar, B. 2007b, Ap&SS, 312, 279
Kushvah, B. S., Sharma, J. P., & Ishwar, B. 2007c, Earth Moon and Planets, 101, 55
Miyamoto, M., & Nagai, R. 1975, PASJ, 27, 533
Murray, C. D. 1994, Icarus, 112, 465
Papadakis, K. E. 2005, Ap&SS, 299, 129
Papadakis, K. E., & Kanavos, S. S. 2007, Ap&SS, 310, 119
Poynting, J. H. 1903, MNRAS, 64, 525
Ragos, O., & Zafiropoulos, F. A. 1995, A&A, 300, 568
Robertson, H. P. 1937, MNRAS, 97, 423
Szebehely, V. 1967, Theory of orbits. The restricted problem of three bodies (New York: Academic Press)
Yeh, L.-C., & Jiang, I.-G. 2006, Ap&SS, 306, 189